

Supplementary Materials

SM1: Membrane fluctuations

Planar geometry

The classical derivation of the membrane fluctuation spectrum is reproduced here, for the case of a planar continuous membrane with tension and bending modulus. This is useful in order to clarify the notation as used in the main text. In the main text this treatment is extended further, to obtain quantities that are observable experimentally. We follow Helfrich's notation (1), and consider a fluctuating membrane of lateral size L whose displacement $h(x, y)$ relative to the average height of the plane is small compared to the lateral size of the fluctuation. The energy cost due to both stretching and bending can be written as:

$$\delta E = \int_0^L \int_0^L \left\{ \frac{\sigma}{2} \left[\left(\frac{\partial h}{\partial x} \right)^2 + \left(\frac{\partial h}{\partial y} \right)^2 \right] + \frac{\kappa}{2} \left[\frac{\partial^2 h}{\partial x^2} + \frac{\partial^2 h}{\partial y^2} \right]^2 \right\} dx dy \quad (\text{S1})$$

where σ is the membrane tension, κ is the bending elastic modulus, and the area of the membrane is $A = L \times L$. By considering each mode as a superposition of Fourier components,

$$\begin{aligned} h(\vec{x}) &= \frac{A}{(2\pi)^2} \int d\vec{q} h_{\vec{q}} e^{i\vec{q}\cdot\vec{x}} \\ \text{with } h_{\vec{q}} &= \frac{1}{A} \int d\vec{x} h(\vec{x}) e^{-i\vec{q}\cdot\vec{x}}, \end{aligned} \quad (\text{S2})$$

and assuming equipartition of energy, the mean square amplitude of each mode can be calculated as (1):

$$\langle h_{\vec{q}}^2 \rangle = \frac{k_B T}{A} \frac{1}{\sigma q^2 + \kappa q^4}, \quad (\text{S3})$$

where $q^2 = q_x^2 + q_y^2$, T is the absolute temperature, and k_B is the Boltzmann constant.

It should be noted for clarity that the direct and inverse Fourier transforms can be defined with arbitrary prefactors (different authors choose preferred normalisations, and Eq. S2 is a common one, used by Helfrich and others), therefore care has to be taken when comparing the ‘‘square amplitudes’’ $h_{\vec{q}}^2$ (as shown in Figure SM1) between papers. It is $h_{\vec{q}}^2$ times

the density of modes which is the physical quantity comparable between different publications.

This form is correct in the limit of small amplitude oscillations, and for flat open membranes. It has been shown that for all but the lowest modes, this formula can be applied to the modes of a quasi-spherical membrane (2). There is however an important aspect to be considered when experiments are done tracking the position of the spherical contour, this is described briefly below.

Equatorial projection

Video microscopy is one of the techniques often used to measure membrane fluctuations. The vesicle is usually visualised along the y axis (from above or below), focussing on the equatorial plane (x, z plane). The edge shows up as a quasi-circular contour, which is detected by image analysis as described in the main text. As first pointed out by Pecreaux *et al.* (2), under these conditions the fluctuations of the contour are described by the Helfrich theory outlined above, but the displacements are related to the Fourier transform of Eq. S3 in the y -coordinate, evaluated at the plane $y = 0$, giving Eq. 1 in the main text. For large q_x , the contour fluctuation spectrum is described by

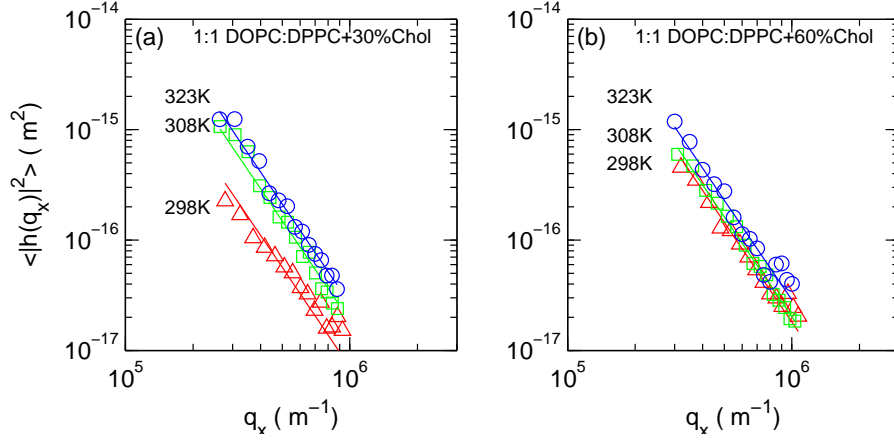
$$\langle h(q_x, y = 0)^2 \rangle = \frac{1}{4L} \frac{k_B T}{\kappa q_x^3}, \quad (\text{S4})$$

where L is simply $2\pi\langle r \rangle$.

Case of complete circumference

This case is used to analyse either homogeneous quasispherical vesicles, or phase-separated vesicles in the early spinodal decomposition regime where they still retain their overall quasispherical shape (see Figure 2 a, b). Typical circumferences are approximately 1000 pixels in length, and we discretize the circular angle into 360 parts ($n = 360$, Figure 2b). The mean radius of curvature $\langle r \rangle$ is calculated as the average of $r(\theta_n)$ over all frames and all θ_n . We then have, for each frame, a set of discrete amplitudes: $h_n = r(\theta_n) - \langle r \rangle$, which are Fourier transformed (using the FFT algorithm in Matlab) to give a set of complex Fourier coefficients c_k :

$$c_k = \sum_{n=1}^N h_n e^{-i2\pi(k-1)(n-1)/N}. \quad (\text{S5})$$



Supplementary Figure SM1: The mean square amplitude of fluctuation modes versus the equatorial wave vector q_x . Data from vesicles of two different compositions and quasi-spherical shape are shown in (a) and (b). Symbols (Δ , \square , \circ) identify increasing temperatures, as noted on the plots. The solid lines correspond to fits of the data using Eq. S4.

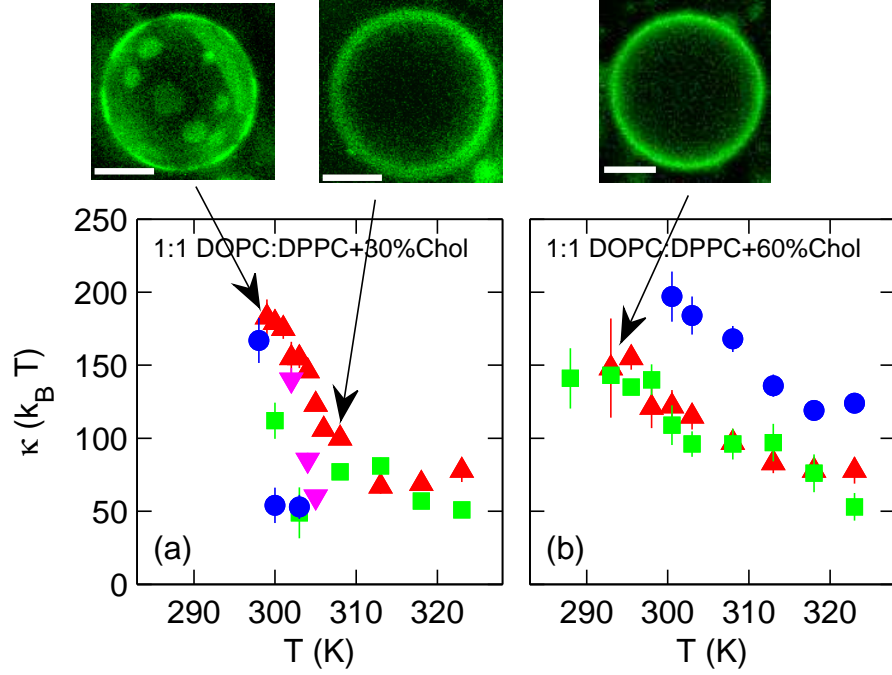
These are the amplitudes of the modes with $q_x^{(k)} = k/\langle r \rangle$, with $k = 1, 2, \dots, +N/2$. The relation between the experimentally determined discrete series c_k and the continuous Fourier transform of h (as in Eq. S4) is given by:

$$h_q^2 = c_k^2 \times \left(\frac{1}{N} \right)^2. \quad (\text{S6})$$

The bending modulus κ is obtained from the experimental data by fitting Eq. S4 in conjunction with Eq. S6, as shown in Figure SM1.

Case of incomplete circumference

Our approach in analysing the membrane fluctuations for the situation of a vesicle morphology consisting of two sections of spheres (with different radii) is similar to the one recently reported in ref (3). The neck region between the spherical sections extends to only a few microns (3, 4), and is not used in this analysis. Choosing vesicles oriented so that the equatorial section is made of two arcs, the fluctuations of the two sections can be analysed separately as

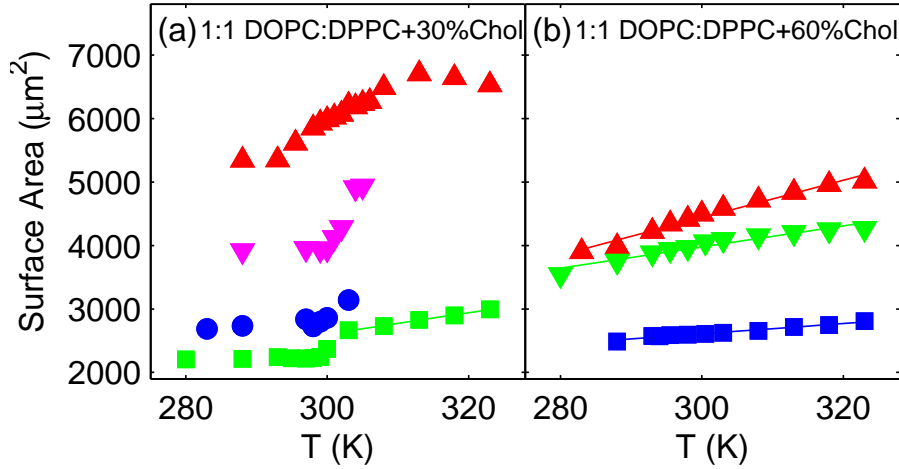


Supplementary Figure SM2: The bending rigidity κ as a function of temperature for several ternary membranes (GUVs) of different composition: (a) 1:1 DOPC:DPPC+30% cholesterol, (b) 1:1 DOPC:DPPC+60% cholesterol. Phase separation is evident at low temperatures for the 30% cholesterol vesicle. The scale bar in the images is $20 \mu\text{m}$. The data in SM1 panels (a) and (b) is from the dataset with marker (Δ).

described above, provided that the amplitude is normalised appropriately to account for the incomplete perimeter. If only an arc under angle θ is selected for analysis, then the mean square amplitude $\langle h'(q_x, y=0)^2 \rangle$ is given by:

$$\langle h'(q_x, y=0)^2 \rangle = \left(\frac{2\pi}{\theta} \right) \frac{1}{4L} \frac{k_B T}{\kappa q_x^3} \quad (\text{S7})$$

where L is the complete circumference $2\pi\langle r \rangle$ as before, and the wavenumber range is reduced to $q'_{xk} = \frac{1}{\langle r \rangle} \left(\frac{2\pi}{\theta}, \frac{2\pi}{\theta} + 1, \dots, \frac{2\pi}{\theta} + \frac{N}{2} \right)$, i.e. part of the low fre-



Supplementary Figure SM3: Surface area of quasi-spherical vesicles, derived from the vesicle diameter, as a function of temperature, for the same experiments shown in SM2 (matching markers). (a) 1:1 DOPC:DPPC+30% cholesterol, (b) 1:1 DOPC:DPPC+60% cholesterol. The sudden changes in diameter in the data in panel (a) correlate with the transition temperature observed simultaneously by microscopy. No phase separation was observed for the vesicles containing 60% cholesterol, panel (b). The solid lines on selected datasets are linear fits, from which the thermal expansion coefficient is calculated, see text. The thermal history is not important, these data were taken on both heating and cooling cycles, and showed no hysteresis.

quency range is lost but the high end and the resolution in q_x is maintained. The normalisation in Eq. S7 can be understood by considering the selection of an arc as a “zero padding” of the function h_n . The control experiments to confirm this analysis are described in the main text.

SM2: Quasi-spherical composite membranes

We analyse the mechanical properties of the membrane immediately after the transition takes place. Figure SM2 shows the dependence of the membrane bending modulus on the temperature, on a short time scale after the onset of the phase separation process, i.e. when numerous micrometre sized domains freely diffuse in the plane of the membrane. For each of the analysed vesicles, we found that upon lowering the temperature the bending

rigidity for the membrane composed of 1:1 DOPC:DPPE + 30%mol cholesterol increased markedly at around 30°C, see Figure SM2(a). The transition temperature was slightly different for different vesicles, most probably due to variations in the membrane composition (see below). The trend clearly indicates a discontinuity in the value of the bending modulus which correlates with the onset of the liquid-liquid phase separation. For the system containing 60%mol cholesterol, where no such phase transformation takes place, the bending modulus shows a weaker dependence on temperature with no sudden jumps, Figure SM2(b). At the lowest temperatures investigated, 10 and 15°C, the fluctuations of the GUVs are below our resolution and the bending modulus cannot be quantified using this technique. Nevertheless, Figure SM2 shows that we can measure values of the bending modulus over $\sim 200 k_B T$ at lower temperatures. It was possible to measure these high values because of the relatively large size of our vesicles, for which the q_x -range is correspondingly shifted to small values. According to Eq. S4, the fluctuation amplitudes decay very rapidly: a factor of 2 in the q_x -range corresponds to almost an order of magnitude in the experimental signal amplitude.

It should be remarked that although the simple mode analysis is ill posed for the case of heterogeneity over lengthscales similar to fluctuation wavelength (as here for the composite membranes, in the phase separated state during coarsening), Figure SM1 does not show any “anomaly”, and the simple homogeneous membrane spectra fits the data very well.

At high temperatures, the vesicles we investigated have bending moduli around $50 k_B T$, with one of the vesicles (Figure SM2(b), square markers) showing a significantly higher value beyond the measurement errors, probably due to bi- or multi-lamellarity. The fact that a mixture of vesicles with various thicknesses is produced is well documented in the literature (5). There is no simple way to distinguish unilamellar vesicles using phase contrast images, except from the flickering amplitude itself. The measured values of the bending modulus for these homogeneous membranes are not very different from the bending rigidity of pure DPPE bilayers above the melting transition, reported to be between 29 and $36 k_B T$ (6, 7) with values as high as $73 k_B T$ also registered using the electro deformation method (8). The addition of cholesterol is also known to increase the phosphocholine bilayer bending rigidity (2, 9). We are not aware of any measurements reported in the literature of the bending modulus of ternary mixtures of this composition in their homogeneous state.

We emphasize the transient, non-equilibrium character of the phase separated membrane, which eventually proceeds towards a complete separation into two large similarly-sized domains on a time scale of tens of minutes.

The recording of fluctuations occurs on a shorter timescale, so we are able to acquire the membrane fluctuation spectrum and extract a value for the bending modulus. The length scale of the bending fluctuations we probe in the phase separated system (set by the q_x -range investigated) are typically between 6 and 20 μm and are therefore comparable or greater than the domain size, so we are typically probing the bending of a heterogeneous membrane. This raises the question about the physical meaning of the bending modulus thus obtained which can only be defined correctly for each separate lipid phase. By applying the standard method for homogeneous membranes we interpret the fluctuation spectra in terms of an ‘effective’ membrane bending modulus. A similar approach has been used before. For example, the first micropipette experiments on active membranes (vesicles with reconstituted bacteriorhodopsin) (10, 11) interpreted the magnification in the membrane fluctuations due to the activity of the protein in terms of an ‘effective’ bending modulus (11) (or, equivalently, an ‘effective temperature’ (10)) by using the standard analysis for passive membranes. Whilst such an effective quantity cannot represent a true material parameter, it is a useful measure for the *overall* changes in the membrane mechanical behaviour due to the onset of phase separation: the suppression of the fluctuation in the separated membrane is a certain sign of the overall stiffening of the membrane. The effective bending modulus of the phase separated membrane will depend not only on the individual bending rigidity for the L_o and the L_α phases, but also on the line tension and the exact membrane morphology (e.g., domain shape, size and distribution) and will slowly vary with time as the domains coarsen and segregate. Nevertheless, we expect the effective bending modulus in the phase separated system to be more sensitive to the mechanical properties of the continuous phase. The higher bending rigidity is thus easily anticipated since the L_o phase is rich in the saturated lipid DPPC (see below for a comparison of the bending moduli). From existing data at 20°C it is known that the composition of the continuous L_o phase is around 1:9 DOPC:DPPC + 40%mol cholesterol (12). The most straightforward interpretation of our results is that the ordered L_o phase has a higher bending modulus than the liquid disordered L_α phase.

This conclusion is confirmed in the direct study of the two separate phases (see main text). The L_o phase is seen to have a higher bending modulus, and has a stronger temperature dependence. We would like to emphasize here the necessity of further experimental and theoretical work in order to fully quantify the mechanical properties of phase-separated membranes. Future experiments should be aimed at investigating how different fluctuation modes can be affected due to the micrometer domain structure. These

studies should be underpinned by a thorough theoretical description of the thermal fluctuation spectrum in heterogeneous membranes, which should take into account the different bending rigidity of the two (or more) types of domains, the effect of the line tension and the exact lateral membrane mesostructure.

SM3: Thermal area expansion

Changes in the vesicle mean area can be quantified from captured contours, which allows the characterisation of membrane thermal expansivity. The mean vesicle diameter was monitored and found to increase by about 10% from 10 to 50°C. SM3 shows the temperature dependence of the vesicle surface area (obtained from the measured mean diameters) for the dataset of quasi-spherical vesicles shown in SM2. These experiments were conducted following different thermal paths. We did not find any systematic dependence on the thermal path, i.e. both the bending modulus and the vesicle diameter were independent of the vesicle thermal history. The mean diameter of the GUVs with 30% cholesterol shows a jump upon crossing the phase boundary, as seen in SM3a. Vesicles containing 60% cholesterol show a continuous expansion, albeit with a similar overall change over the entire temperature range. To further characterize the membrane properties, we measured the membrane thermal expansion coefficient, $\beta = (1/A_0)(dA/dT)$, from the linear parts of the temperature dependencies of the vesicle area (see SM3 for the lines of best fit). For vesicles containing 60% cholesterol, SM3(b), the experimentally obtained values are $(7.6 \pm 0.9) \times 10^{-3} \text{ K}^{-1}$, $(4.7 \pm 1.0) \times 10^{-3} \text{ K}^{-1}$, and $(3.3 \pm 0.8) \times 10^{-3} \text{ K}^{-1}$. A similar value, $(6.3 \pm 0.6) \times 10^{-3} \text{ K}^{-1}$, is also obtained for the system containing 30% cholesterol, SM3(a), above the critical temperature (in the L_α phase). These values are typical for the thermal expansivity of lipid bilayers in liquid-crystalline state. As a comparison, the reported value of the thermal expansion coefficient for dimyristoylphosphocholine (DMPC) bilayers is $6.8 \times 10^{-3} \text{ K}^{-1}$ at about 5°C above the main phase transition (stearoyloleoylphosphocholine (SOPC) bilayers show a lower thermal expansivity of $3.3 \times 10^{-3} \text{ K}^{-1}$) (13). The value of the apparent thermal expansion coefficient for the phase separated membrane (SM3(a) below the critical temperature) is significantly reduced to $(0.4 \pm 1.0) \times 10^{-3} \text{ K}^{-1}$, which seems to reflect the changes in the lipid and cholesterol-lipid interactions in the newly formed L_0 phase.

The diameter change upon crossing the phase boundary from coexisting liquids to a uniform liquid state could possibly lead to an increase in the available excess area, resulting in a deviation from the spherical shape. Vice

versa, for a vesicle equilibrated above T_c , cooling could lead to the onset of membrane tension. We did not observe such transitions in the data reported in Figure SM2, but such a possibility cannot be ruled out at lower temperatures where the fluctuation amplitudes are below our resolution.

References

1. Helfrich, W., and R. M. Servuss, 1984. Undulations, steric interaction and cohesion of fluid membranes. *Nuovo Cimento D* 3:137–151.
2. Pecreaux, J., H. G. Dobereiner, J. Prost, J. F. Joanny, and P. Bassereau, 2004. Refined contour analysis of giant unilamellar vesicles. *Eur. Phys. J. E* 13:277–290.
3. Semrau, S., T. Idema, L. Holtzer, T. Schmidt, and C. Storm, 2008. Accurate determination of elastic parameters for multicomponent membranes. *Phys. Rev. Lett.* 100:088101.
4. Julicher, F., and R. Lipowsky, 1996. Shape transformations of vesicles with intramembrane domains. *Phys. Rev. E* 53:2670–2683.
5. Hackl, W., U. Seifert, and E. Sackmann, 1997. Effects of Fully and Partially Solubilized Amphiphiles on Bilayer Bending Stiffness and Temperature Dependence of the Effective Tension of Giant Vesicles. *J. Phys. II (France)* 7:1141–1157.
6. Lee, C. H., W. C. Lin, and J. P. Wang, 2001. Using differential confocal microscopy to detect the phase transition of lipid vesicle membranes. *Opt. Eng.* 40:2077–2083.
7. Fernandez-Puente, L., I. Bivas, M. D. Mitov, and P. Meleard, 1994. Temperature and Chain Length Effects on Bending Elasticity of Phosphatidylcholine Bilayers. *Europhys. Lett.* 28:181–186.
8. Mishima, K., S. Nakamae, H. Ohshima, and T. Kondo, 2001. Curvature elasticity of multilamellar lipid bilayers close to the chain-melting transition. *Chem. Phys. Lipids* 110:27–33.
9. Evans, E., and W. Rawicz, 1990. Entropy-driven tension and bending elasticity in condensed-fluid membranes. *Phys. Rev. Lett.* 64:2094–2097.

10. Manneville, J. B., P. Bassereau, D. Levy, and J. Prost, 1999. Activity of Transmembrane Proteins Induces Magnification of Shape Fluctuations of Lipid Membranes. *Phys. Rev. Lett.* 82:4356–4359.
11. Manneville, J. B., P. Bassereau, D. Levy, and J. Prost, 2000 In Giant Vesicles, Luisi, P. L. and Walde, P., Eds. and J. Wiley and Sons; Chapter 27.
12. Cicuta, P., S. L. Keller, and S. L. Veatch, 2007. Diffusion of Liquid Domains in Lipid Bilayer Membranes. *J. Phys. Chem. B* 111:3328.
13. Evans, E., and D. Needham, 1987. Physical properties of surfactant bilayer membranes: thermal transitions, elasticity, rigidity, cohesion, and colloidal interactions. *J. Phys. Chem.* 91:4219–4228.